VIP Polymer Chemistry Very Important Paper

International Edition: DOI: 10.1002/anie.201505790
German Edition: DOI: 10.1002/ange.201505790

Conductive Elastomers with Autonomic Self-Healing Properties

Kun Guo, Da-Li Zhang, Xiao-Mei Zhang, Jian Zhang, Li-Sheng Ding, Bang-Jing Li, and Sheng Zhang**

Abstract: *Healable, electrically conductive materials are highly desirable and valuable for the development of various modern electronics. But the preparation of a material combining good mechanical elasticity, functional properties, and intrinsic self-healing ability remains a great challenge. Here, we design composites by connecting a polymer network and single-walled carbon nanotubes (SWCNTs) through host–guest interactions. The resulting materials show bulk electrical conductivity, proximity sensitivity, humidity sensitivity and are able to self-heal without external stimulus under ambient conditions rapidly. Furthermore, they also possess elasticity comparable to commercial rubbers.*

All synthetic materials suffer damage during their functional lifetimes. The development of self-healing materials that are able to repair themselves spontaneously after mechanical damage improves the reliability, safety, and environmental impact of man-made materials.[1,2] Up to now, most work has been done on self-healing structural materials, which restore their mechanical properties by mending the mechanical damage.[3–7] Only few attempts have been made to materials which are able of restoring other functional properties, such as conductivity.[8–18]

Electrically conductive materials are a kind of functional material and are indispensable for the development of various modern electronics. The conductive healable materials could be applied in many advanced electronics such as electronic skin, electrical conductors, and batteries, and improve the reliability of these devices greatly. For example, irreversible healing-type electrical materials that have exciting applications for electrical conductors were developed by using healed capsules as healing agents.[9–12] When a mechanical damage was exerted to the capsules, these capsules were ruptured and the conductive species were released to the damaged region and restored the conductivity. This capsule-based method is fast, efficient, and the healing process is autonomous. But the healing is not repeatable at a given place. Reversible healing-type electrical materials are fabricated by introducing reversible bonds to conductive composites. Because the broken reversible bonds at the damaged area are able to reform, the composites restore their mechanical and electrical properties.[13–15] In these cases, intrinsical self-healing without external aid is very difficult. For example, we have reported a kind of conductive composite composed of small molecules and nanotubes recently. Although these composites can rapidly heal electrical and mechanical properties several times, the healing processes need the aid of water.[16] Bao and co-workers have developed spontaneously healing materials based on hydrogen bonds,[13,17] but they still suffers from the poor tolerance to moisture. In addition, although a good elasticity is highly desirable for the development of advanced organic electronic devices, among the few examples of self-healing conductive materials, elastic materials are very scarce.[18]

Here, emphasis was put on the development of a conductive elastomer with autonomic healing ability. We describe self-healing conductive composites by combining poly(2-hydroxyethyl methacrylate) (PHEMA) and single-walled carbon nanotubes (SWCNTs) through host–guest interactions. This PHEMA-SWCNT composite combines bulk electrical conductivity, proximity sensitivity, humidity sensitivity and is able to self-heal under ambient conditions without external stimulus. Furthermore, it also possesses elasticity comparable to commercial rubbers. This elasticity will significantly expand the application scope of self-healing conductive materials, particularly for the electronics capable of undergoing significant deformation.

Figure 1 a shows the preparation procedure of the material. SWCNTs were selected as conductive filler providing conductivity to the composite. The surface of the SWCNTs was decorated by β-cyclodextrin (β-CD) using π–π interactions between SWCNT and pyrene-modified β-CD, enabling the organic SWCNTs to interact with an adamantine (Ad) modified polymer matrix through host–guest interactions. UV/Vis-NIR spectra and fluorescence spectra (Supporting information Figure S1) show the π–π stacking between pyrene groups of Py-β-CD and SWCNTs.[19] Thermogravimetric analysis (TGA) results show that the weight percentage of β-CD in Py-β-CD/SWCNT hybrids was 72.9 wt % (see Figure S2 in the Supporting Information). The resulting Py-β-CD-SWCNT can be dispersed in aqueous solution, forming a homogeneous and stable suspension for several months (Figure S3). In contrast, the original SWCNTs precipitated in water immediately.

The PHEMA-SWCNT composite was prepared in a two-step process: 1) self-assembly of Py-β-CD-SWCNT and Ad-modified 2-hydroxyethyl methacrylate (HEMA-AD) and

[*] K. Guo, X. Zhang, Prof. Dr. L. Ding, Prof. Dr. B. Li
Key Laboratory of Mountain Ecological Restoration and Bioresource Utilization, Chengdu Institute of Biology
Chinese Academy of Sciences, Chengdu, 610041 (China)
E-mail: libj@cib.ac.cn

D. Zhang, Prof. Dr. S. Zhang
State Key Laboratory of Polymer Materials Engineering
Polymer Research Institute of Sichuan University
Sichuan University, Chengdu, 610065 (China)
E-mail: zslbj@163.com

Prof. Dr. J. Zhang
School of Chemistry and Chemical Engineering
Shanxi University, Taiyuan, 030012 (China)

Supporting information for this article is available on the WWW under http://dx.doi.org/10.1002/anie.201505790.

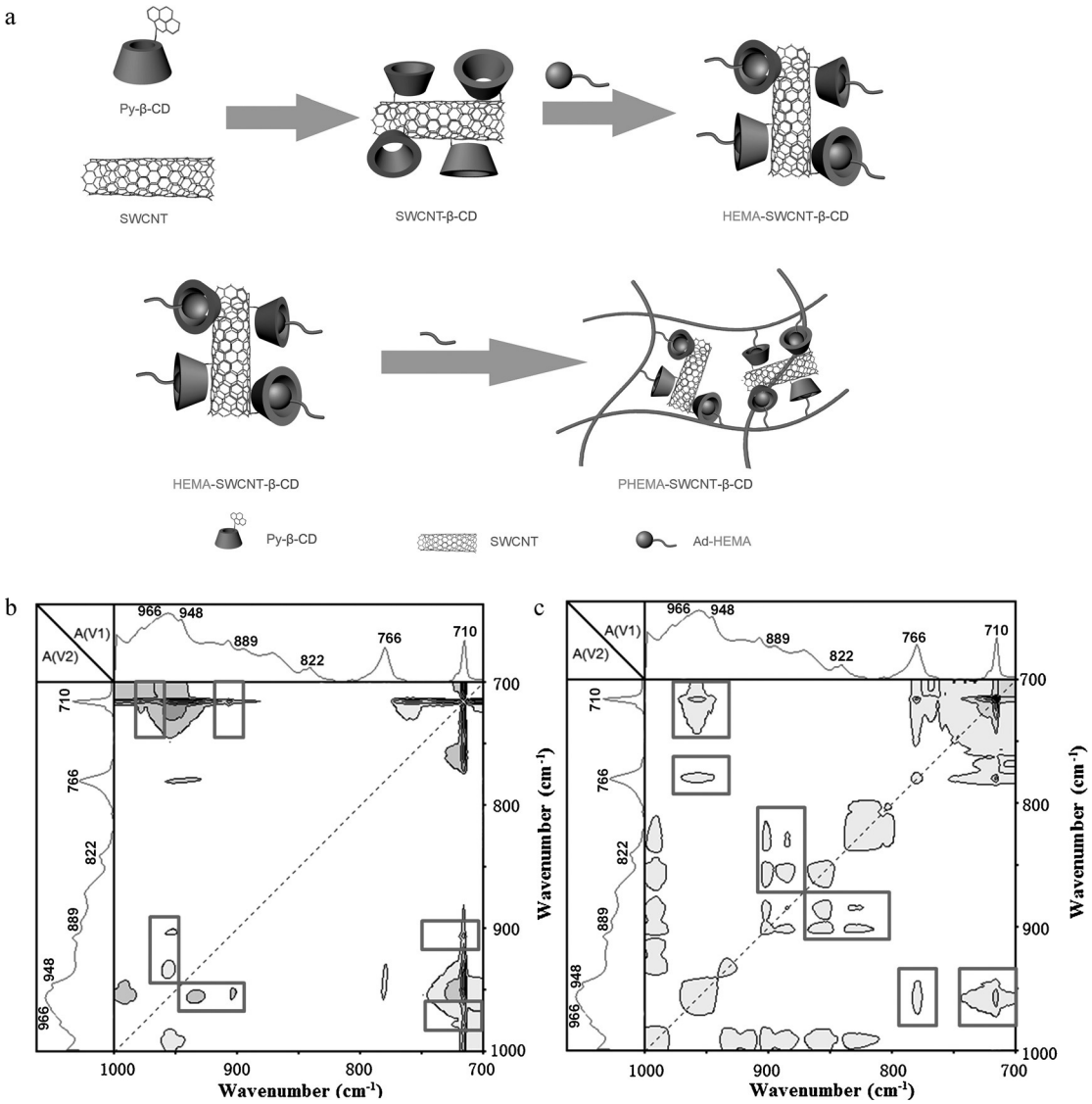

Figure 1. a) Preparation of PHEMA-SWCNT composites. b) Synchronous and c) asynchronous 2D correlation spectra of the PHEMA-SWCNT composite (SWCNT 10 wt%) in the 700–1000 cm^{-1} region constructed from 25–70 °C. The gray boxes represent the signals of β-CD correlated with the resonance of the Ad groups.

2) crosslinking Py-β-CD-SWCNT/HEMA-AD and HEMA monomer. β-CD could interact with adamantane and its derivatives to form stable inclusion complexes.[20,21] Therefore, by mixing the Py-β-CD/SWCNT and HEMA-AD together in DMSO/H_2O (V/V = 9:1) solution, inclusion complexes were formed because of the interaction between AD and β-CD moieties. TGA results confirmed that the HEMA-AD was attached to the Py-β-CD/SWCNT (Figure S2). 2D NMR NOESY spectra showed an obvious correlation between the signals of the β-CD and AD groups, demonstrating that the AD groups were threaded through the cavity of β-CD moieties to form inclusion complexes (Figure S4c).[22–24] The crosslinking of HEMA and the inclusion complexes was obtained by free-radical polymerization using ethylene glycol dimethacrylate (EGDMA) as crosslinker.[25] The resulting materials were homogeneous rubber-like materials.

The formation of a crosslinked PHEMA-SWCNT composite and the interaction between Ad and β-CD in the composite were investigated by two-dimensional infrared (2D IR) spectroscopy , which has been proved a powerful tool for studying the molecular interactions in many systems.[26] Figure 1 b shows the synchronous 2D correlation spectra of a SWCNT/PHEMA complex at 700–1000 cm^{-1} constructed at a temperature range from 25 to 70 °C (for clarity, not all of the spectra are shown). Typical features of HEMA (1702 and 1450 cm^{-1}), Ad (966 and 889 cm^{-1}) and β-CD (755 and 705 cm^{-1}) are shown simultaneously,[27,28] indicating the formation of a crosslinked PHEMA-SWCNT composite. More importantly, features of Ad and β-CD also obviously showed a correlation, while this cross-peak almost disappeared in the physical mixture of SWCNTs-β-CD and HEMA-Ad map (Figure S5). According to the theory for 2D IR spectroscopy developed by Noda,[29] a correlation peak is generated when two dipole transition moments associated with molecular vibrations of different functional groups are reorienting simultaneously. Such cooperative motion of the local struc-

tures is expected when strong interactions exist among different groups. These results indicated that Ad and β-CD moieties in the PHEMA-SWCNTs composite strongly interacted with each other owing to the formation of inclusion complexes. As a control sample, a PHEMA/SWCNT blend sample (10 wt% SWCNT) in which the SWCNT was not covered by β-CD was also prepared. But the SWCNTs precipitated during polymerization of HEMA, resulting in a heterogeneous distribution of the SWCNTs.

All the PHEMA-SWCNT composites behaved similarly to rubber under ambient conditions, and can flex into various conformations easily (Figure S6). Detailed mechanical properties of the composites are summarized in Table S1. Increasing the amount of SWCNT resulted in a decrease of the maximum strain and an increase of Young's modulus.[30] But even when the weight percentage of the SWCNT was up to 20%, the elongation at the break of the sample was 325%, comparable to the values of conventional rubber (e.g. soft polydimethylsiloxane).[31–33] Moreover, we carried out loop tests for a PHEMA-SWCNT composite (10% SWCNT). Figure 2a shows the stress–strain curves of sample through sequential extension/retraction cycle of varying maximum stretch. The loading paths show the typical rubber-like behavior. The unloading curves show a pronounced hysteresis loop with a permanent set, suggesting the composite dissipated energy effectively.[34,35]

Figure 2b shows the DSC curves of the PHEMA-SWCNT composites. The glass-transition temperature (T_g) values of all of the samples were below room temperature (20°C), confirming that they were in the rubbery state at room temperature. The T_g of the PHEMA-SWCNT composites increased gradually with increasing amount of SWCNTs, owing to the fact that the SWCNT acted as macro-crosslinker to increase the crosslinking degree of the composites.

The cross-sectional scanning electron microscopy (SEM) image of PHEMA-SWCNT (10 wt% SWCNT) revealed that the SWCNTs randomly entangled to form a high density of junctions (Figure 2c), which is the key factor in the conductivity of the PHEMA-SWCNT composite. As shown in Table S2, the conductivity of samples increased with increasing amount of SWCNTs. When the weight percentage of SWCNT was up to 20%, the conductivity of the material was

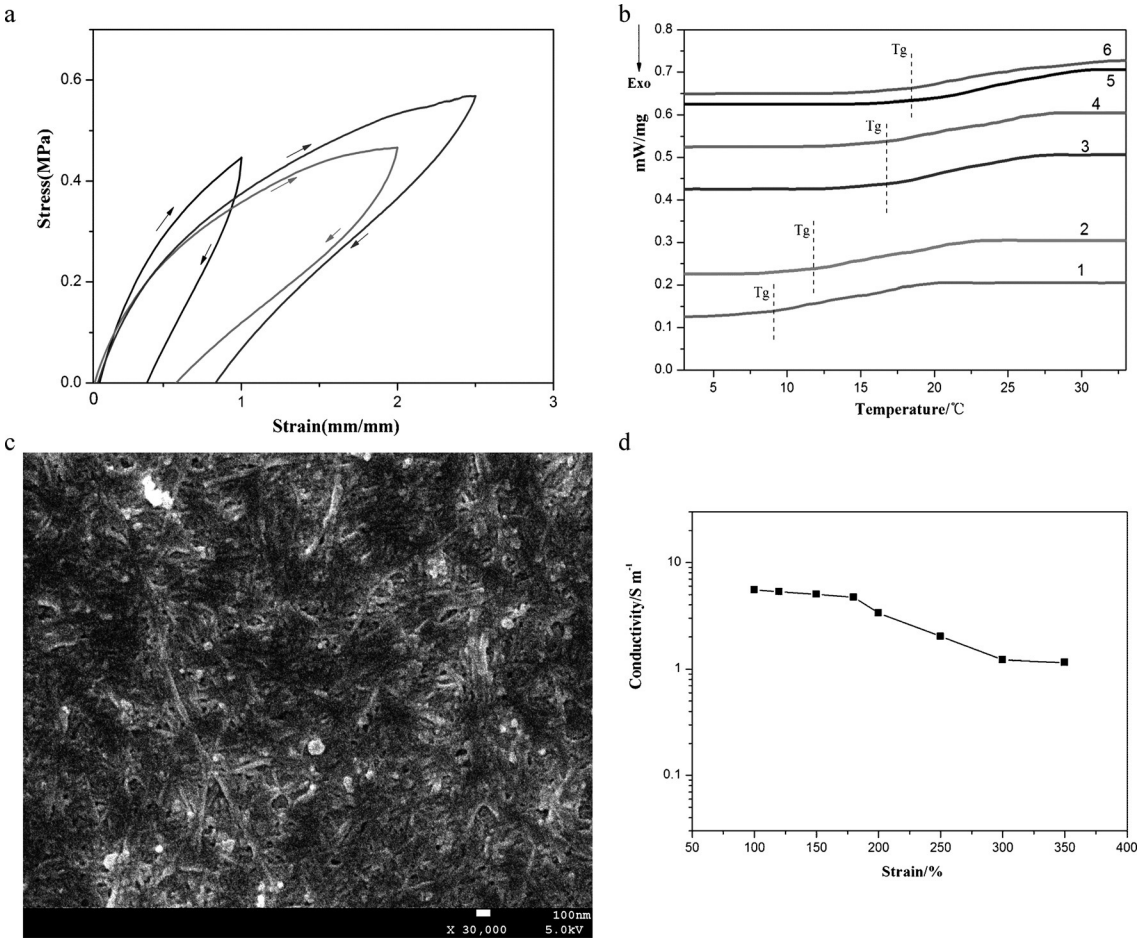

Figure 2. a) PHEMA-SWCNT composites (10 wt% SWCNT) were subjected to a cycle of loading and unloading of varying maximum stretch. b) Differential scanning calorimetric (DSC) analysis of all the composites with various SWCNT content. (Sample 1 (SWCNT 0 wt%), T_g = 8.4°C, sample 2, (SWCNT 6 wt%), T_g = 12.1°C, sample 3 (SWCNT 7 wt%), T_g = 15.1°C, sample 4, (SWCNT 8 wt%), T_g = 16.3°C, sample 5, (SWCNT 10 wt%), T_g = 16.9°C, sample 6, (SWCNT 20 wt%), T_g = 17.1°C). c) Cross-sectional SEM image of the self-healing composites with 10 wt% SWCNT (scale bar = 100 nm). d) The conductivity of the PHEMA-SWCNT composite (SWCNT 10 wt%) under uniaxial extension at deformations up to 350% strain.

7.76 S m^{-1} under ambient lab condition, slightly lower than that of SWCNTs (10.98 S m^{-1}). Furthermore, it was found that the conductivity of the PHEMA-SWCNT sample was almost kept constant and independent of the distance between the probes, implying a homogenous distribution and a lack of phase aggregation of the nanotubes in the composite owing to the hydrophilicity of β-CD. The control sample, a PHEMA/SWCNT blend sample (10 wt% SWCNT) in which the SWCNTs were not covered by β-CD, was an insulator because SWCNTs were distributed heterogeneously and failed to construct a conductive pathway even if their contents was above the percolation threshold. Therefore, the light-emitting diode (LED) did not shine when this control sample was connected to a circuit with a LED lampion and a power source (Figure S7a).

Figure 2d shows the conductivity of the PHEMA-SWCNT composite (SWCNT 10 wt%) under uniaxial extension at deformations up to 350% strain. It can be seen that the conductivity of the samples did not show significant changes when uniaxially stretched by 180% or less. Under large strain, the conductivity decreased moderately. But even when the strain was 350%, the conductivity of materials still remained at the same order of magnitude with the result of an unstretched sample. The loss of conductivity at a large extension is due to a partial breakdown of the SWCNT network, which leads to a decrease in the total number of conduction paths. A similar trend of conductivity loss was observed for all composites with a different SWCNT amount (Figure S7b).

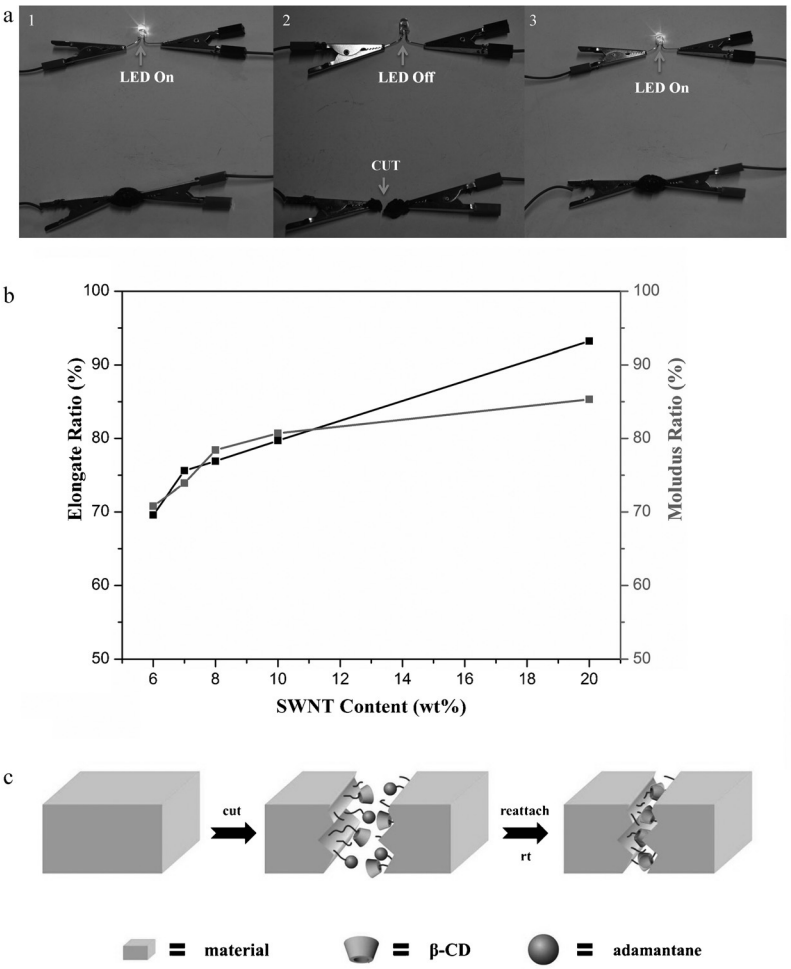

Figure 3. a) Demonstration of the electrical healing process for the PHEMA-SWCNT composite: 1) as-prepared PHEMA-SWCNT composite specimen (SWCNT 10 wt%) connected in a circuit with a LED. 2) The specimen was cut to break the circuit. 3) The LED was shining again after the specimen was healed. b) Elongate ratio and modulus ratio of the original and healed composites with different SWCNT contents. c) Schematic illustration of self-healing of the PHEMA-SWCNT composite.

We speculated that the PHEMA-SWCNT composites would show a self-healing property due to the large number of host–guest interactions in the systems. As a proof-of-concept demonstration for electrical healing, a PHEMA-SWCNT composite sample was connected to a circuit with a LED lampion and a power source (the voltage was set to 4.5 V).[36] As shown in Figure 3a, the LED was shining when the amount of SWCNTs in the PHEMA-SWCNT composite was above 7 wt%. After cutting the PHEMA-SWCNT sample into two pieces, the LED went off immediately. Then gently bringing the cut pieces back into contact, the specimen self-healed after only 5 minutes under ambient conditions without any treatment, and the LED turn on again (Movie S1). The conductivities of PHEMA-SWCNT composites after healing were measured across the healed cut. As shown in Table S2, the electrical healing efficiency for all specimens with a different amount of SWCNT was nearly 95%. These results indicated that most conduction paths reformed after the healing. As a control test, the PHEMA/SWCNT blend specimen (in which the SWCNTs were not functionalized by β-CD) was not able to self-heal (Figure S8), although interdiffusion of the PHEMA across the interfaces may occur. This result suggested that interactions between β-CD and Ad played a key role for the self-healing. Moreover, we performed a test and described the time evolution of a typical electrical healing process (Figure S9). It was found that the conductivity suddenly jumped when the cut composite pieces are put back together.

Unlike the recovery of conductivity, the recovery of the mechanical properties took a couple of minutes. The strain was almost restored by over 90% and the stress recovered by more than half after 5 minutes. After less than 5 minutes, the recovery of the mechanical properties was obviously worse. After more than 5 minutes, the mechanical healing efficiency did not increase significantly (Figure S10). The SWCNTs contents in the composites also affected the mechanical healing efficiency. As shown in Figure 3b, the mechanical healing efficiency increases with increase in the mass fraction of SWCNTs. The higher the SWCNT-β-CD content is, the more host–guest interactions are at the damaged interface, enabling efficient healing capability. The partial mechanical healing may be due to the fact that not only reversible

interactions were broken, and a lot of covalent bonds were also broken as the sample was damaged. Multiple cuts on previous scars did not cause significant strength loss further. After the first self-healing cycle, the strength of the PHEMA-SWCNT composite (10 wt% SWCNT) was 70.1 kPa. After the third cycle, the strength was still 66.7 kPa (Figure S11).

To further analyze the self-healing mechanism, we designed three control tests: we soaked the cut pieces in β-CD solution, pyrene-modified α-CD (Py-α-CD) solution, and deionized water for 5 minutes, respectively. In β-CD solution, the host–guest interactions between the damaged interface should be hindered, because free β-CDs were able to act as competitive hosts hindering the formation of inclusion complexes between the guest and β-CD moieties in the sample.[37,38] In the Py-α-CD solution, the π–π interactions between damaged interfaces should be shielded, because the Py groups in Py-α-CD were able to connect with the Py groups or the nanotubes at the damaged interface easily. Interestingly, healing was not observed for the cut pieces soaked in β-CD solution. On the contrary, the separated cut pieces soaked in deionized water and Py-α-CD solution healed automatically when they were reattached for 5 minutes (Movies S2, S3 and Figures S12, S13). The above results indicated that the host–guest interactions are the healing motif of PHEMA-SWCNT composites, and π–π interactions did not play the dominant role for healing. Figure 3c shows the schematic illustration of self-healing of the PHEMA-SWCNT composite. When a PHEMA-SWCNT composite sample was cut into pieces, many Ad-β-CD links were broken near the cut surface because their strength (99 pN)[39] was lower than that of covalent bonds. These non-associated groups were "eager" to link together, therefore, Ad-β-CD reformed across the interface when the broken pieces were pressed together. As a result, the sample self-healed.

We also investigated the influence of healing conditions on the self-healing ability of PHEMA-SWCNT composites. Unlike the observation of a hydrogen-bonded self-healing system, the separation time did not negatively affect the healing efficiency. Longer waiting times between the cut and re-contact result in the absorption of moisture, which cause a loss of the hydrogen-bonding ability but a benefit for the host–guest inclusion complexation.[16] Actually the PHEMA-SWCNT composites turned rigid and lost the self-healing ability after the samples were dried in vacuum for 48 h at 45 °C. It is difficult to realize an assembly process through host–guest interactions between rigid blocks because the surface roughness causes a distance between the blocks which is beyond the supramolecular interactive distance.[40] Hydrogen-bonding between the polymer chains conferred strength to the polymer and the polymer chains lost mobility when water of the PHEMA-SWCNT composites was lost, leading to insufficient host–guest bonding between two objects. A decreased healing temperature below T_g of PHEMA-SWCNT composites also decreased the mobility of the polymer chains and resulted in a loss of the self-healing ability. The PHEMA chains easily absorb water from the air, so the PHEMA-SWCNT composites showed healing ability even in a very dry environment (relative humidity, RH, 20%) at room temperature.

The PHEMA-SWCNT composites showed moisture absorption capacity under ambient condition because of the hydrophilicity of the hydroxy groups. As shown in Figure 4a,

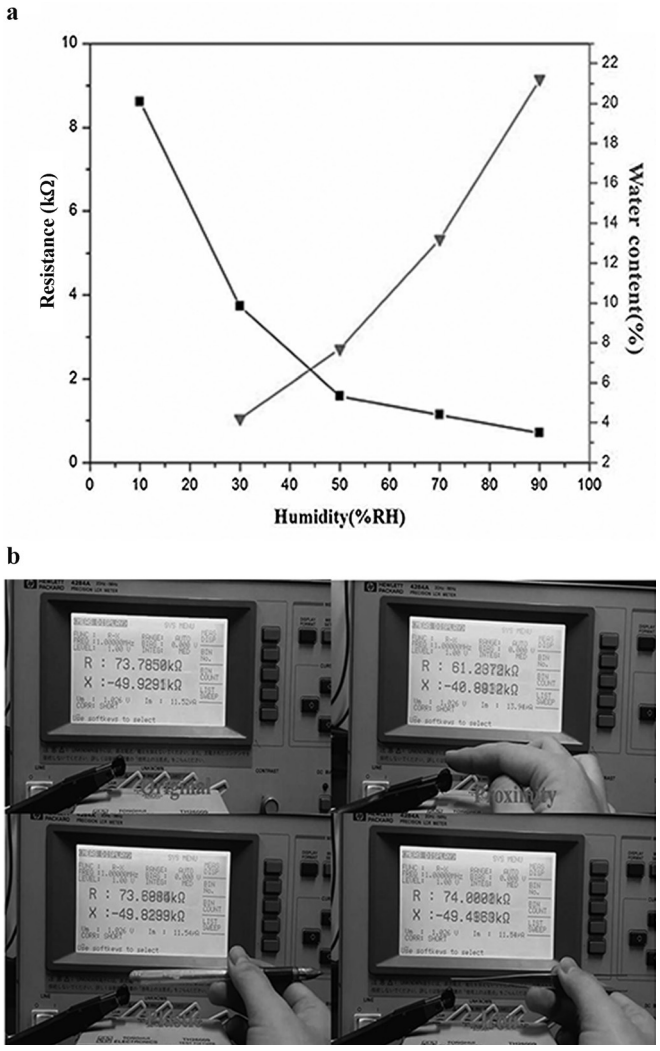

Figure 4. a) The relationship between relative humidity and water content and the influence of humidity on the resistance. b) The proximity sensing was performed by a finger, plastic, and iron.

the water absorption of the PHEMA-SWCNT composites (size: $10 \times 10 \times 10$ mm) increased with increasing RH. Because of the moisture absorption capacity the resistance of the composites was sensitive to the RH of the environment. The resistance of samples was around 8.62 kΩ in dry air (RH 10%), which was about 2 or 6 times that in air of 30 or 60% RH (Figure 4a), respectively. Using this humidity-sensitive property, a humidity sensor based on the PHEMA-SWCNT composite can be fabricated. As far as we know, up to now, most conductive materials used as moisture sensor did not show a self-healing property.[41,42]

The PHEMA-SWCNT composites also can be used for proximity sensing. As shown in Movie S4, placing a finger

near the PHEMA-SWCNT composite (10 wt% SWCNT) caused a change in the resistance. The finger can be detected within a distance of 5 mm with an excellent response and recovery time interval. However, the composite did not react to conducting (iron) and insulating (plastic) materials (Figure 4b, Figure S14). Similar phenomena also were observed in a cellulose nanocrystal/reduced graphene oxide film.[43] These observations were attributed to the electrically conducting nature of the human body. The skin tissue displays a certain electric field, as the finger comes closer to the surface of the sensor material, and the fringe electric field produced by the material is disturbed because of a tiny electric charge transfer from the finger, inducing fluctuations in the resistance.[43–46] This human skin recognition capacity of PHEMA-SWCNT composites makes them good candidates for smart robotics.

This work demonstrates a new design strategy for self-healing functional materials by connecting functional inorganic particles (such as SWCNT) and a polymer network through host–guest interactions. The resulting materials combine the high elasticity of the polymer network and the conductivity of the SWCNT, have autonomic healing ability owing to the host–guest interactions, and show interesting proximity and humidity sensitivity. Therefore, these functional materials have a high potential for building advanced sensing electronics. Furthermore, considering that many other functional particles, such as magnetic fluid particles, and quantum dots, could also easily modified by CD, a wide range of functional systems with spontaneously healing properties are expected to be produced using the design concept developed herein.

Acknowledgements

This work was supported by National Natural Science Foundation of China (grant number 5137374), CAS Knowledge Innovation Program (grant number KSCX2-EW-J-22), and West Light Foundation of CAS.

Keywords: conductivity · elastomers · host–guest interactions · nanotubes · self-healing properties

How to cite: *Angew. Chem. Int. Ed.* **2015**, *54*, 12127–12133
Angew. Chem. **2015**, *127*, 12295–12301

[1] M. Zhang, D. Xu, X. Yan, J. Chen, S. Dong, B. Zheng, F. Huang, *Angew. Chem. Int. Ed.* **2012**, *51*, 7011–7015; *Angew. Chem.* **2012**, *124*, 7117–7121.
[2] X. Yan, D. Xu, X. Chi, J. Chen, S. Dong, X. Ding, Y. Yu, F. Huang, *Adv. Mater.* **2012**, *24*, 362–369.
[3] I. Bond, S. White, N. Sottos, *J. R. Soc. Interface* **2007**, *4*, 347–348.
[4] H. Jin, C. L. Mangun, A. S. Griffin, J. S. Moore, N. R. Sottos, S. R. White, *Adv. Mater.* **2014**, *26*, 282–287.
[5] J. A. Syrett, C. R. Becer, D. M. Haddleton, *Polym. Chem.* **2010**, *1*, 978–987.
[6] Y. Chen, A. M. Kushner, G. A. Williams, Z. Guan, *Nat. Chem.* **2012**, *4*, 467–472.
[7] S. Chen, X. Li, Y. Li, J. Sun, *ACS Nano* **2015**, *9*, 4070–4076.
[8] H. Sun, Y. Xiao, Y. Jiang, G. Guan, X. Fang, J. Deng, P. Chen, Y. Luo, H. Peng, *Angew. Chem. Int. Ed.* **2014**, *53*, 9526–9531; *Angew. Chem.* **2014**, *126*, 9680–9685.
[9] S. A. Odom, S. Chayanupatkul, B. J. Blaiszik, O. Zhao, A. C. Jackson, P. V. Braun, N. R. Sottos, S. R. White, J. S. Moore, *Adv. Mater.* **2012**, *24*, 2578–2581.
[10] M. M. Caruso, S. R. Schelkopf, A. C. Jackson, A. M. Landry, P. V. Braun, J. S. Moore, *J. Mater. Chem.* **2009**, *19*, 6093–6096.
[11] S. A. Odom, M. M. Caruso, A. D. Finke, A. M. Prokup, J. A. Ritchey, J. H. Leonard, S. R. White, N. R. Sottos, J. S. Moore, *Adv. Funct. Mater.* **2010**, *20*, 1721–1727.
[12] B. J. Blaiszik, S. L. B. Kramer, M. E. Grady, D. A. Mcllroy, J. S. Moore, N. R. Sottos, S. R. White, *Adv. Mater.* **2012**, *24*, 398–401.
[13] C. Wang, H. Wu, Z. Chen, M. McDowell, Y. Cui, Z. Bao, *Nat. Chem.* **2013**, *5*, 1042–1048.
[14] H. Wang, B. Zhu, W. Jiang, Y. Yang, W. R. Leow, H. Wang, X. Chen, *Adv. Mater.* **2014**, *26*, 3638–3643.
[15] Y. Li, S. Chen, M. Wu, J. Sun, *ACS Appl. Mater. Interfaces* **2014**, *6*, 16409–16415.
[16] D. Zhang, X. Ju, L. Li, Y. Kang, X. Gong, B. Li, S. Zhang, *Chem. Commun.* **2015**, *51*, 6377–6380.
[17] B. C. Tee, C. Wang, R. Allen, Z. Bao, *Nat. Nanotechnol.* **2012**, *7*, 825–832.
[18] Y. Li, S. Chen, M. Wu, J. Sun, *Adv. Mater.* **2012**, *24*, 4578–4582.
[19] T. Ogoshi, Y. Takashima, H. Yamaguchi, A. Harada, *J. Am. Chem. Soc.* **2007**, *129*, 4878–4879.
[20] T. Kakuta, Y. Takashima, A. Harada, *Macromolecules* **2013**, *46*, 4575–4579.
[21] M. Nakahata, Y. Takashima, A. Hashidzume, A. Harada, *Angew. Chem. Int. Ed.* **2013**, *52*, 5731–5735; *Angew. Chem.* **2013**, *125*, 5843–5847.
[22] C. Moers, L. Nuhn, M. Wissel, R. Stangenberg, M. Mondeshki, E. B. Nicoletti, A. Thomas, D. Schaeffel, K. Koynov, M. Klapper, R. Zentel, H. Frey, *Macromolecules* **2013**, *46*, 9544–9553.
[23] J. Liu, J. Alvarez, W. Ong, E. Román, A. E. Kaifer, *J. Am. Chem. Soc.* **2001**, *123*, 11148–11154.
[24] W. Ha, Y. Kang, S. Peng, L. Ding, S. Zhang, B. Li, *Nanotechnology* **2013**, *24*, 495103–495110.
[25] R. Fuhrer, E. K. Athanassiou, N. A. Luechinger, W. J. Stark, *Small* **2009**, *5*, 383–388.
[26] D. E. Rosenfeld, Z. Gengeliczki, B. J. Smith, T. D. P. Stack, M. D. Fayer, *Science* **2011**, *334*, 634–639.
[27] Q. Liu, C. Li, T. Yang, T. Yi, F. Li, *Chem. Commun.* **2010**, *46*, 5551–5553.
[28] R. C. Sabapathy, S. Bhattacharyya, W. E. Cleland, C. L. Hussey, *Langmuir* **1998**, *14*, 3797–3807.
[29] I. Noda, *J. Am. Chem. Soc.* **1989**, *111*, 8116–8118.
[30] C. Wang, N. Liu, R. Allen, J. B. H. Tok, Y. Wu, F. Zhang, Y. Chen, Z. Bao, *Adv. Mater.* **2013**, *25*, 5785–5790.
[31] M. V. Circu, Y. S. Ko, A. C. Gerecke, D. M. Opris, *Macromol. Mater. Eng.* **2014**, *299*, 1126–1133.
[32] J. Lessing, S. A. Morin, C. Keplinger, A. S. Tayi, G. M. Whitesides, *Adv. Funct. Mater.* **2015**, *25*, 1418–1425.
[33] J. Biggs, K. Danielmeier, J. Hitzbleck, T. Kridl, S. Nowak, E. Orselli, X. Quan, D. Schapeler, W. Sutherland, J. Wagner, *Angew. Chem. Int. Ed.* **2013**, *52*, 9409–9421; *Angew. Chem.* **2013**, *125*, 9581–9595.
[34] L. Xia, R. Xie, X. Ju, W. Wang, Q. Chen, L. Chu, *Nat. Commun.* **2013**, *4*, 2226–2236.
[35] J. Sun, X. Zhao, W. R. K. Illeperuma, O. Chandhuri, K. H. Oh, D. J. Mooney, J. J. Vlassak, Z. Suo, *Nature* **2012**, *489*, 133–136.
[36] S. Benight, C. Wang, J. Tok, Z. Bao, *Prog. Polym. Sci.* **2013**, *38*, 1961–1977.
[37] M. Nakahata, Y. Takashima, H. Yamaguchi, A. Harada, *Nat. Commun.* **2011**, *2*, 511–516.
[38] Y. Wang, D. Zhang, T. Zhou, H. Zhang, W. Zhang, L. Luo, A. Zhang, B. Li, S. Zhang, *Polym. Chem.* **2014**, *5*, 2922–2927.

[39] A. Gomez-Casado, H. H. Dam, D. Yilmaz, D. Florea, P. Jonkheijm, J. Huskend, *J. Am. Chem. Soc.* **2011**, *133*, 10849 – 10857.
[40] M. Cheng, F. Shi, J. Li, Z. Lin, C. Jiang, M. Xiao, L. Zhang, W. Yang, T. Nishi, *Adv. Mater.* **2014**, *26*, 3009 – 3013.
[41] Q. Kuang, C. Lao, Z. Wang, Z. Xie, L. Zheng, *J. Am. Chem. Soc.* **2007**, *129*, 6070 – 6071.
[42] J. Feng, L. Peng, C. Wu, X. Sun, S. Hu, C. Lin, J. Dai, J. Yang, Y. Xie, *Adv. Mater.* **2012**, *24*, 1969 – 1974.
[43] K. K. Sadasivuni, A. Kafy, L. Zhai, H. Ko, S. Mun, J. Kim, *Small* **2015**, *11*, 994 – 1002.
[44] S. Mao, S. Cui, G. Lu, K. Yu, Z. Wei, J. Chen, *J. Mater. Chem.* **2012**, *22*, 11009 – 11013.
[45] S. Y. Liew, W. Thielemans, D. A. Walsh, *J. Phys. Chem. C* **2010**, *114*, 17926 – 17933.
[46] S. Kim, W. Choi, W. Rim, Y. Chun, H. Shim, H. Kwon, J. Kim, I. Kee, S. Kim, S. Y. Lee, J. Park, *IEEE Trans. Electron Devices* **2011**, *58*, 3609 – 3615.

Received: June 23, 2015
Revised: July 27, 2015
Published online: August 25, 2015

